

# Flight-Determined Multivariable Stability Analysis and Comparison of a Control System

John J. Burken\*

NASA Dryden Flight Research Facility, Edwards, California 93523

Singular value analysis can give conservative stability margin results. Applying structure to the uncertainty can reduce this conservatism. This paper describes flight-determined stability margins for the X-29A lateral-directional, multiloop control system. These margins are compared with the predicted unscaled structured singular values, scaled structured singular values, and conventional single-loop phase and gain margins. The algorithm was further evaluated with flight data by changing the roll-rate-to-aileron-command-feedback gain by  $\pm 20\%$ . Minimum eigenvalues of the return difference matrix that bound the singular values are also presented. Extracting multiloop singular values from flight data and analyzing the feedback gain variations validates this technique as a measure of robustness. This analysis can be used for near-real-time flight monitoring and safety testing.

## Nomenclature

$A$	= general matrix
$D$	= scaling matrix
$e$	= actuating signal error vector
$G_{gs\_ \delta_a}$	= ground-generated signal (GGS) telemetered from ground to aileron path
$G_{gs\_ \delta_r}$	= GGS telemetered from ground to rudder path
$G(s)$	= plant transfer function matrix
$h$	= altitude, ft
$HG$	= loop gain matrix
$H(s), H(z)$	= controller transfer function matrices, $z = e^{sT}$
$K_2$	= roll-rate-to-aileron-feedback gain, deg/(deg/s)
$L$	= perturbation matrix
$M$	= Mach number
$S_{uu}$	= autospectrum of input
$S_{xu}$	= cross spectrum of input-to-output
$u$	= external input command vector
$X_u$	= control transfer function matrix
$x$	= control system output vector
$y$	= plant output vector
$\delta_a$	= aileron position
$\delta_{a\_cmd}$	= aileron command to actuator, deg
$\delta_r$	= rudder position
$\delta_{r\_cmd}$	= rudder command to actuator, deg
$\lambda$	= eigenvalue
$\lambda_{analy}$	= analytical minimum eigenvalue
$\lambda_{flt}$	= in-flight minimum eigenvalue
$\sigma$	= singular values, $\sigma_n = \sqrt{\lambda_n(A^*A)}$
$\sigma_{flt}$	= in-flight minimum singular value
$\sigma_{SSV}$	= analytical structured singular values (SSV)
$\sigma_{USV}$	= analytical unscaled structured singular values (USV)

## Introduction

MULTIVARIABLE control systems have been used for decades; however, the methodology to evaluate the stability margins was not developed until the last decade.<sup>1</sup> Classical frequency  $\omega$  analysis methods, such as Bode or Nyquist techniques, work well for single-input/single-output (SISO) systems but are inadequate for multiple-input/multiple-output (MIMO) control systems. Classical methods do not allow for simultaneous variations of phase and gain in all of the feedback paths.<sup>1-3</sup> Recently, singular value  $\sigma$  norms of the return difference matrix (RDM) have been considered a measure of the system stability margin for multiloop feedback control systems.<sup>1,2,4</sup> However, singular value norms of systems with unstructured uncertainty can be overly conservative, and a control system designer could interpret the results as unsatisfactory when, in fact, the system is robust.<sup>3</sup> A method for relieving the excessive conservatism is derived by structuring the uncertainties.<sup>2,3,5</sup>

Although mathematically sound, singular value methods require substantial evaluation using multiloop control systems before these methods can be accepted as adequate for determining the robustness of control system design. Some insight into application of experimentally determined singular values of a multiloop flutter suppression control system for a wind-tunnel aeroelastic model has been reported.<sup>6</sup> Singular values of the RDM at the input and output locations were used successfully to evaluate the performance of the control system, and computations were given for the open-loop transfer matrix  $GH$  from open-loop control system wind-tunnel operations.<sup>6</sup> This research concentrated on wind-tunnel aeroelastic control performance; however, evaluation is also needed for USV and scaled SSV methods for analyzing multiloop control systems of manned aircraft in flight. In addition, theoretical and flight-determined stability margins need to be compared.

To evaluate the stability of an in-flight multiloop system, NASA Dryden Flight Research Facility conducted a flight test program on a MIMO flight control system using the X-29A aircraft. This aircraft is designed to test the feasibility of integrating several modern technologies into a highly maneuverable aircraft with a thin supercritical 30 deg forward-swept wing and close-coupled canards.<sup>7-9</sup> Longitudinal control of the aircraft is achieved with canard, symmetric flaperons, and strake surfaces. Lateral-directional motion is controlled by a multiloop system with conventional rudder and differential flaperon deflection.

This paper extends the previously reported method<sup>6</sup> by determining singular values from flight data, comparing these values with the predicted or analytical USV and SSV,  $\sigma_{USV}$  and

Presented as Paper 92-4396 at the AIAA Guidance, Navigation, and Control Conference, Hilton Head, SC, Aug. 10–12, 1992; received Sept. 23, 1992; revision received March 1, 1993; accepted for publication March 8, 1993. Copyright © 1992 by the American Institute of Aeronautics and Astronautics, Inc. No copyright is asserted in the United States under Title 17, U.S. Code. The U.S. Government has a royalty-free license to exercise all rights under the copyright claimed herein for Governmental purposes. All other rights are reserved by the copyright owner.

\*Aerospace Engineer, Dynamics and Control Branch, Mail Stop D4840D, P.O. Box 273, Member AIAA.

$\sigma_{SSV}$ , and presenting the classical predicted SISO frequency response analysis. Flight results of the minimum eigenvalues  $\lambda$  obtained from the RDM and comparisons with the analytical minimum eigenvalues  $\lambda_{analy}$  are also presented. To determine the sensitivity of the MIMO stability margin algorithm, a lateral-directional X-29A control system feedback gain was changed. Several flight conditions were flown and analyzed, but for the sake of brevity, one representative case is reported here. The flight test results are for three control law gain settings of the roll-rate-feedback gain at a flight condition of  $M = 0.7$  and  $h = 30,000$  ft. The technique described in this paper can be used to obtain near-real-time stability margins during flight for multiloop control systems.

### Control System Description

A ground-based computer linked by telemetry transmission to the X-29A flight control system remotely excites the aircraft dynamics with sweeps, step inputs, and doublets. This GGS system is used to repeat maneuvers, provide for independent control surface inputs, and produce well-defined inputs for frequency response calculations. The GGS, aileron, and rudder commands to the actuator are the only digital flight control system signals needed for this MIMO analysis. These signals were integrated with other data from a data bus and downlinked to the ground at 40 samples/s. The measured data were relatively noise free because the response paths included antialiasing filters.<sup>10</sup>

The X-29A aircraft has a triplex digital flight control system with an analog backup for each channel. Digital control law outputs are computed at 40 Hz in dual-processor flight computers. Because the longitudinal flight control system is a SISO system, it is not evaluated in this paper.

Figure 1 shows a simplified linearized block diagram of the X-29A lateral-directional control system. Pilot stick-shaping and feed-forward dynamics are not included because they have no impact on closed-loop stability. The GGS, aileron, and rudder commands to the actuator are included in this figure. The four aircraft-filtered feedback signals are roll rate  $p$ , yaw rate  $r$ , roll attitude  $\phi$ , and lateral acceleration  $N_y$ . Roll-rate-to-aileron-feedback gain  $K2$ , a function of flight condition, is the only gain that could be changed in flight that had any impact on the closed-loop stability margins. This gain could only be changed by  $\pm 20\%$  of the nominal value to determine the sensitivity of the singular value algorithm. The pilot could change the control system software  $K2$  in flight by selecting a set of predetermined gains.

### Analytical Methods

The  $\sigma_{USV}$  method can be too conservative, and the results could be interpreted as unsatisfactory when, in fact, the stability margins are adequate. The scaled  $\sigma_{SSV}$  method decreases the conservative nature of singular values. Both methods of determining the analytical multivariable stability margins are discussed in this section. Background information on stability margins using singular values, analytical unscaled and scaled structured singular values, eigenvalue analysis, and singular values analysis of flight data are also presented. Classical

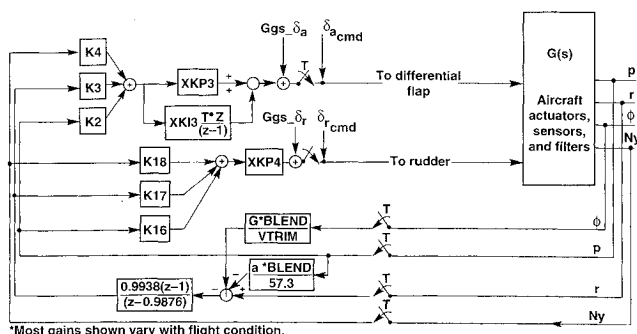


Fig. 1 Simplified X-29 lateral-directional control system.

SISO stability margins are presented in the Results and Discussion section.

### Stability Margins Using Singular Values

Singular values of the RDM are used to measure the stability margins.<sup>1-4</sup> This analysis provides in a minimum sense the uncertainty that can be tolerated in all the loops simultaneously before a multivariable system becomes unstable. The RDM at the input node is  $[I + HG]$ . At the output node, the RDM is  $[I + GH]$ . As the minimum singular value  $\sigma$  of the input or output RDM approaches zero, the system becomes increasingly less stable.

To analyze the RDM, a review of the general singular value analysis is helpful. Let  $A$  be a general  $[n \times n]$  matrix, then the minimum and maximum singular values  $\bar{\sigma}$  are

$$\underline{\sigma}[Ax] = \min \|Ax\| \equiv \sqrt{\lambda_{\min}[A^*A]} \quad (1)$$

$$\|x\| = 1$$

$$\bar{\sigma}[Ax] = \max \|Ax\| \equiv \sqrt{\lambda_{\max}[A^*A]} \quad (2)$$

$$\|x\| = 1$$

where  $\|\cdot\|$  is the Euclidean norm,  $\lambda[\cdot]$  are the eigenvalues, and  $A^*$  is the conjugate transpose of matrix  $A$ . Note that vector  $Ax$  depends on the units of vector  $x$ ; therefore, the singular values also depend on the scale units of  $x$  variables.<sup>2</sup> Other useful properties of singular values are as follows<sup>2,3</sup>:

$$\underline{\sigma}[A^{-1}] = 1/\bar{\sigma}[A] \quad (3)$$

$$\underline{\sigma}[A] \leq |\lambda[A]| \leq \bar{\sigma}[A] \quad (4)$$

Equation (4) states that the magnitude of the eigenvalues of  $A$  is bounded by the minimum and maximum singular values of  $A$ .

Figure 2 shows a typical analytical control system. The  $L_i$  and  $L_o$  represent the input and output perturbation matrices. The MIMO systems have crossfeed interactions that cause the locations of perturbations to affect the singular value results. In classical SISO systems, locations of the disturbances are unimportant. Ignoring the perturbation matrices for now, the relationships of the RDM for the input node  $[I + HG]$  and the output node  $[I + GH]$  are usually different. Therefore, the singular values are different because matrix multiplication is not commutative, i.e.,  $GH \neq HG$ .

If the multiloop system is stable when unperturbed, then a sufficient but not necessary condition for the system to remain stable when  $L_i$  is perturbed is that<sup>2,11,12</sup>

$$\bar{\sigma}(L_i^{-1} - I) < \underline{\sigma}[I + H(j\omega)G(j\omega)] \quad (5)$$

When analyzing the input node, the output perturbation matrix is set to identity,  $L_o = I$ . The right-hand side of Eq. (5),  $\underline{\sigma}[I + HG]$ , is the minimum singular value of the input node RDM and is used as the basis of this robustness analysis. Analysis of singular values will work for SISO systems for

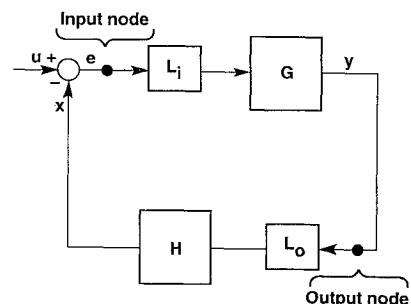


Fig. 2 Control diagram with disturbance matrices at the input and output nodes.

determining stability margins.<sup>3</sup> However, the values may not necessarily match the gain and phase margins obtained using the classical definitions because singular value analysis will be conservative.

#### Analytical Unscaled Structured Singular Values

A fully populated perturbation matrix  $L_i$  produces the most conservative stability margins. The robustness of a system with a fully populated  $L_i$  can give an unrealistic measure of the stability margins.<sup>1-3</sup> Often, these perturbations can be adequately defined using the diagonal elements of  $L_i$ . When the  $L_i$  matrix is diagonal, it takes on the structure

$$L_i = \text{diag}[k_1 e^{j\phi_1}, k_2 e^{j\phi_2}, \dots, k_n e^{j\phi_n}] \quad (6)$$

where  $k_i$  is the uncertainty gain element and  $\phi_i$  is the uncertainty phase element of the  $L$  matrix. In addition,  $k_i$  and  $\phi_i$  ( $i = 1, n$ ) may change independently and simultaneously with respect to one another in each control loop. This method allows for the robustness analysis of multivariable control systems.

Now that the ground work has been laid, the system stability boundary can be defined by testing the criterion

$$\sigma[I + HG(j\omega)L_i] = 0 \quad (7)$$

as a function of frequency. This expression is the neutral stability boundary that produces a pure resonance at frequency  $\omega$ . This relationship means that a pole of the closed-loop system on the imaginary axis exists and that the minimum singular value of the RDM is zero. Whether the closed-loop system is stable or unstable, the singular values are always nonnegative, as Eq. (1) indicates. The singular values are magnitudes of a transformation that are always positive and define the distance to the neutral stability boundary.<sup>3</sup> The greater the magnitude of the minimum singular value, the greater the robustness.

One goal of this research was to extend the well-understood, classical stability margin methods from SISO to MIMO controllers. Equation (7) represents the information needed to determine the stability margins of a system. However, in this form, this equation does not relate the magnitude of the minimum singular value to traditional phase and gain margins. The relationship that expresses the gain and phase as a direct function of either the input or output perturbations is shown in Eq. (8), where  $L$  is either  $L_i$  or  $L_o$ .<sup>4</sup>

$$\sigma(L^{-1} - I) = \sqrt{(1 - 1/k_n)^2 + 2/k_n [1 - \cos(\phi_n)]} \quad (8)$$

Figure 3 shows a graphical representation of Eq. (8) and presents minimum singular value as a function of phase and gain margins. To determine the stability margins or nearness to instability, compute  $\sigma[I + HG(j\omega)]$  for various frequencies. The minimum singular value plot traces the nearness to singularity of the RDM and, thus, the system robustness to perturbations. It is not necessary to know the perturbation matrix  $L$  to compute the minimum singular value plot.<sup>3</sup>

#### Analytical Scaled Structured Singular Values

Because the singular values of a fully populated  $L$ -matrix are conservative, it may be misleading to apply these values to a control system. Such values may indicate that the system is not robust. The Analytical Unscaled Singular Values subsection structured the uncertainty by making the  $L$ -matrix diagonal [Eq. (6)]. The USV method reduces the conservatism; however, scaling the system further reduces this conservatism yet also maintains realistic margins.<sup>1,3,5</sup> This reduction is accomplished by including a diagonal scaling matrix  $D$  in the RDM expression. The scaling should be chosen so as to maximize the minimum singular value across the frequency range.

$$\sigma\{I + D(j\omega)[H(j\omega)G(j\omega)]D(j\omega)^{-1}\} \leq \text{SSV} \quad (9)$$

Equation (9) represents the singular values as a function of frequency in the presence of the matrix  $D(\omega)$ , which reduces the sensitivity of cross-feed perturbations. Implementation of the  $D$  matrix minimizes the conservative nature of singular values of multiloop robustness predictions. Equation (9) eliminates the conservatism for control systems where the dimension of  $HG$  is three or less.<sup>5,11</sup> Using the relationship of Eq. (9), the  $D$  matrix scaling produces results that are equivalent to using structured singular values ( $\mu$  analysis) assuming the disturbances are white noise.<sup>12</sup> The predicted singular values of the RDM,  $[I + HG]$  as well as  $[I + DHGD^{-1}]$ , can be determined from linear frequency analysis.

#### Eigenvalue Analysis

As shown in the Stability Margins Using Singular Values subsection, the node point location of the analysis can influence system stability. Note that system singular values will always be upper bounded by the eigenvalues of the RDM [Eq. (4)]. The eigenvalues of the RDM are identical at any location in the control system<sup>6</sup> and can be expressed as

$$\left| \frac{\lambda(I + HG)}{\text{input node}} \right| = \left| \frac{\lambda(I + GH)}{\text{output node}} \right| \quad (10)$$

Equation (10) represents the upper limit of the minimum singular value and, therefore, the upper bounds of the stability margins of a multiloop control system. Plotting the minimum eigenvalues of the RDM along with the singular values can be useful in a qualitative sense. The distance between the  $\sigma$  plot and the  $\lambda$  plot can be viewed as the conservativeness of the singular value analysis.<sup>3</sup> The eigenvalues of the RDM are not the same as those of the closed-loop system.

#### Singular Value Analysis of Flight Data

Flight singular values and eigenvalues need to be determined by using frequency response techniques. This section describes the methodology used to determine singular values from flight test data. Transfer function equation development, eigenvalues, and singular values of the RDM are included.

A complex frequency response of a system can be estimated from the autospectrum and cross spectrum of the input and output time history variables by transforming these time domain responses to the frequency domain using fast Fourier transforms (FFTs). The controller input-to-output,  $[u(t)]$ -to- $[x(t)]$ , transfer matrix (Fig. 2)  $X_u$  is defined as follows:

$$\{X_u(j\omega)\}_{ij} = \sum_{k=1}^N [S_{x_i} u_i(j\omega)]_k [S_{u_i} u_i(j\omega)]_k^{-1} \quad (11)$$

where  $S_{xu}$  is the cross spectrum of the input  $u$  and output  $x$ ,  $S_{uu}$  is the autospectrum of the input, and  $N$  is the number of time history arrays. These data were loaded into arrays of 2048

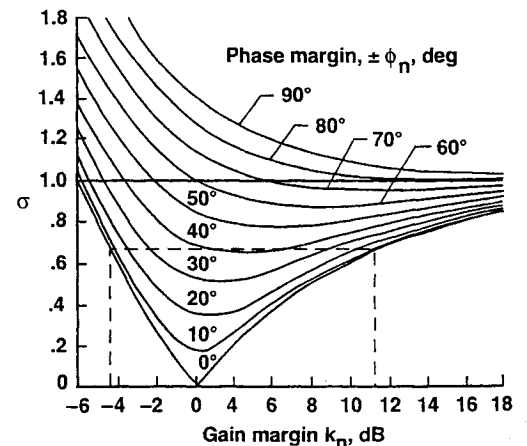


Fig. 3 Universal diagram for multiloop gain-phase margin evaluation.

points. A raised cosine-smoothing window was used to process the time history data obtained from flight. The matrix  $X_u$  is a combination of simple transfer function estimations of input-to-output signals, and for a  $2 \times 2$  system, such as the X-29 input node, the response matrix is

$$X_u(j\omega) = \begin{bmatrix} x_1/u_1 & x_1/u_2 \\ x_2/u_1 & x_2/u_2 \end{bmatrix} \quad (12)$$

Response matrix  $X_u$  can be used to construct the RDM  $[I + HG]$ . Equations (13-16) show the relationship of  $X_u$  to the RDM. Closed-loop system robustness is determined from the minimum singular values of the RDM at either the plant input node  $\sigma[I + HG]$  or the output node  $\sigma[I + GH]$ . Perturbation matrices  $L_i$  and  $L_o$  are not required for flight-determined singular value analysis because variations are inherent in the system dynamics. The scaling matrix  $[D]$  can be used to normalize the units of the response matrix  $[X_u]$  to improve the flight singular values. For the X-29A input node, the commands to the roll axis were of the same order of magnitude as were those to the yaw axis. Therefore, scaling was not attempted or used on flight data. If the singular values were analyzed at the output node, then scaling the flight data would most likely have been used because of the large scaling differences between the output sensors ( $p$ ,  $r$ ,  $\phi$ , and  $N_y$ ). The output node singular values are not presented because there were only two external excitation signals available and four output signals. This situation produces an underdetermined case, and a unique solution was not possible. The following closed-loop relationships can be developed from Fig. 2 if the perturbation matrices are ignored:

$$e = u - x \quad (13)$$

$$x = HGe = HG[u - x] \quad (14)$$

The complex frequency response of the open-loop transfer function can be estimated from the autospectrum and cross spectrum of  $u$  and  $x$ .

$$S_{xu} = HG[S_{uu} - S_{xu}] \quad (15)$$

This relationship can be postmultiplied by the autospectrum inverse  $S_{uu}^{-1}$ .

$$S_{xu}S_{uu}^{-1} = HG[S_{uu}S_{uu}^{-1} - S_{xu}S_{uu}^{-1}] \quad (16)$$

Combining Eqs. (11) and (16) produces

$$X_u = HG[I - X_u] \quad (17)$$

Therefore, the loop gain matrix as a function of frequency is

$$HG(j\omega) = X_u(j\omega)[I - X_u(j\omega)]^{-1} \quad (18)$$

The expressions have now been developed to determine the flight test singular values for the stability margins of multiloop control systems. The spectral relationships of this section can be rapidly evaluated using FFTs, which make it possible to determine, during flight, the near-real-time stability margins of multiloop control systems.

### Flight Test Procedure

Maneuvers flown for the multivariable stability margin analysis were designed to excite the motion of the lateral-directional axis. The pilot stabilized the aircraft at the desired flight condition. Then a GGS frequency sweep would be commanded to the roll axis to excite the X-29A dynamics. The GGS maneuver was completed after approximately 45 s, and the pilot re-established the initial flight condition. Next, the same GGS frequency-sweep signal was commanded to the yaw

axis for approximately 45 s to complete the needed inputs for the transfer function estimation. The GGS frequency-sweep signal started at 40 rad/s and finished at 0.1 rad/s. This signal sweep helped to maintain the initial flight condition without requiring pilot corrections. Ground-generated as well as aileron- and rudder-commands-to-actuator signals were recorded for the MIMO analysis at 40 samples/s during these maneuvers. For the three  $K2$  values, the pilot would dial in the appropriate settings on the control system panel, and the GGS maneuvers were repeated.

### Results and Discussion

This section presents flight results of singular values and compares these results with the analytical USV and SSV as well as classical SISO analyses. The minimum eigenvalues of the RDM and an evaluation of how the singular value analysis algorithm performed are also presented. Figure 4 shows the ground-generated frequency sweep and resulting roll axis time response. Flight singular values were determined using the time history signals from Fig. 4 and similar time histories from the yaw axis.

Figure 5 shows the flight-determined input node minimum singular values  $\sigma[I + HG]$  with the nominal  $K2$  as well as analytical structured and unstructured singular values. This plot shows that good agreement exists between the flight and analytical data. The analytical SSVs tend to agree slightly better with the flight data than with the analytical USVs. This result is consistent with theory.

Figure 6 shows the scaling or structuring used on the analytical system. The dimension of the diagonal  $D$  is  $2 \times 2$ , which is the same size as  $HG$ . The scaling algorithm set the  $D_{22}$  element to 1.0 and left the  $D_{11}$  element free to maximize Eq. (9). As shown in Fig. 6,  $D_{11}$  is the same order of magnitude as  $D_{22}$ ; therefore, the scaling will not have as large an impact on the results as it would if the scaling were to differ by several orders of magnitude. Another point to note is that as the  $D$  matrix approaches unity  $I$ , the SSVs become the same as the USVs. Comparing the minimum singular values in Fig. 5 using the scaling  $D$  elements in Fig. 6 shows that the modeling of the X-29A analytical system was good.

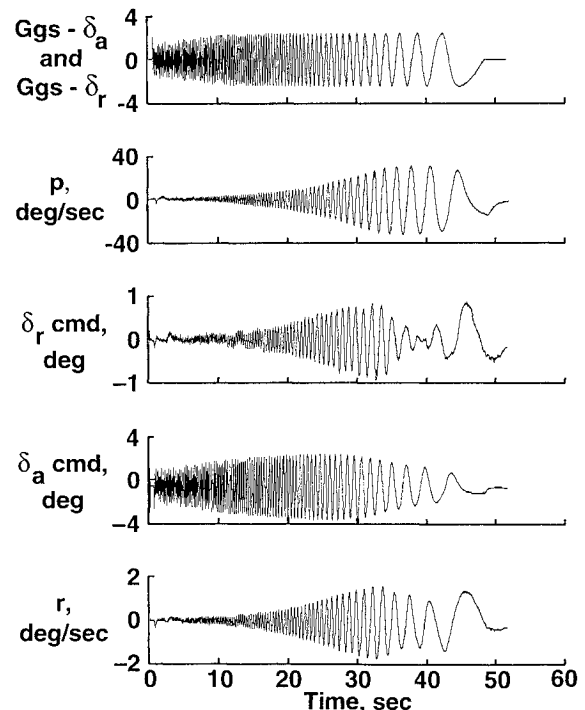


Fig. 4 Ground-generated sweep and roll axis response time histories ( $M = 0.7$ ,  $h = 30,000$  ft, and  $K2 = 100\%$ ).

The minimum flight singular value is 0.72 at 8.0 rad/s (see Fig. 5), and represents the worst closed-loop stability margin. The universal phase and gain margin plot of Fig. 3 is required to relate the  $\sigma = 0.72$  to a stability margin. From Fig. 3, a singular value of 0.72 corresponds to gain margins of  $-4.8$  and  $11.5$  dB and to a phase margin of  $\pm 41$  deg. Dashed lines highlight the area of interest in this figure. These singular values thus imply that the gain in both paths can be increased by  $11.5$  dB or reduced by  $4.8$  dB simultaneously before the system becomes unstable. Similarly, the phase in both paths can be changed by  $\pm 41$  deg before the system becomes unstable. The analytical unscaled minimum singular value is approximately 0.65 at 8 rad/s, which corresponds to a gain margin between  $-4$  and  $8.5$  dB and a phase margin of  $\pm 35$  deg. The SSV method matched the peak and valley of the flight minimum singular values better than the USV method. As expected, analytical USV stability margins were lower or more conservative than analytical SSV margins.

The minimum eigenvalue is the upper bound of the minimum singular value of the RDM, as expressed in Eq. (4).

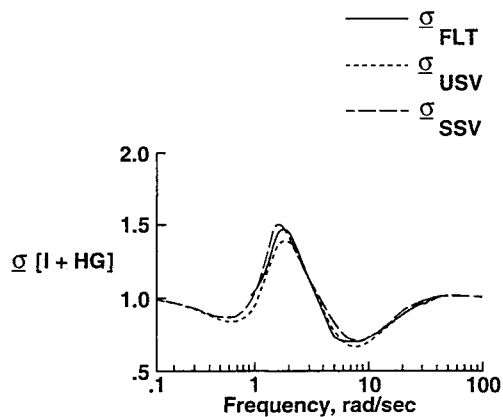


Fig. 5 Flight and predicted minimum singular values ( $M = 0.7$ ,  $h = 30,000$  ft, and  $K2 = 100\%$ ).

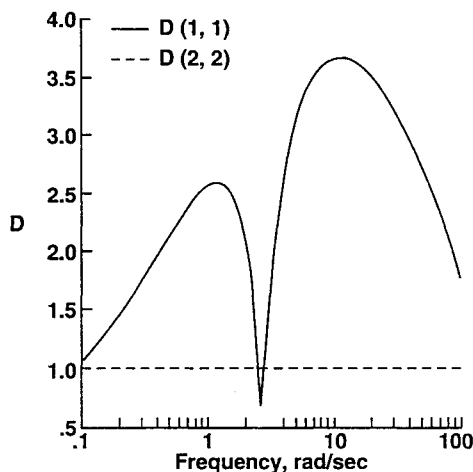


Fig. 6 Diagonal scaling matrix  $D(\omega)$  applied to the input return difference matrix ( $M = 0.7$ ,  $h = 30,000$  ft, and  $K2 = 100\%$ ).

Figure 7 combines the  $\lambda_{\text{fit}}$  and the  $\sigma$  from Fig. 5. The singular value curves are equal to or below the eigenvalue curve, which agrees with Eq. (4) ( $\sigma \leq \lambda$ ).

To investigate the ability of the algorithm to detect a change in stability margins,  $K2$  was changed in flight by  $\pm 20\%$ , and the same flight maneuvers were repeated. For comparison, Fig. 8 shows the three flight-determined singular values for the three  $K2$  settings: 80, 100, and  $120\%$ . The algorithm detected the multiloop stability margin change caused by the single  $K2$  change of  $\pm 20\%$ .

For comparison purposes, the classical single-loop frequency response results (SISO) are shown in Table 1 along with the singular value analysis.

The minimum stability margin determined by the SISO method was  $13$  dB and  $62$  deg, whereas the flight singular value (MIMO) method resulted in a margin of  $11.5$  dB and  $41$  deg. As expected, the singular value method is conservative, but the results between the SISO and MIMO methods are very similar. The X-29A lateral axis is basically uncoupled from the directional axis. At low angles of attack, the roll response does

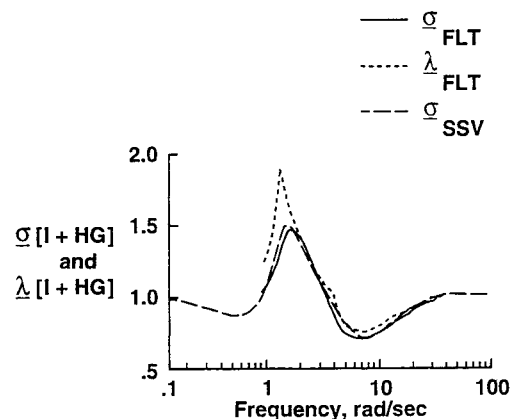


Fig. 7 Flight and predicted minimum singular values and eigenvalues of  $[I + HG]$  ( $M = 0.7$ ,  $h = 30,000$  ft, and  $K2 = 100\%$ ).

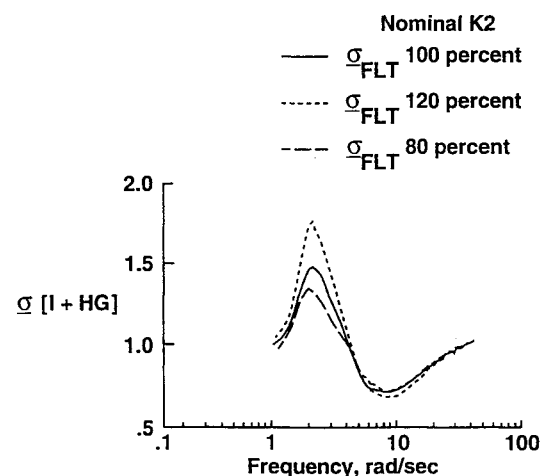


Fig. 8 Flight minimum singular values as a function of gain settings for  $K2 = 120, 100$ , and  $80\%$  ( $M = 0.7$  and  $h = 30,000$  ft).

Table 1 Comparison of SISO and MIMO analysis at Mach 0.7, an altitude of 30,000 ft, and nominal  $K2$

	Multiple-input/multiple output <sup>a</sup>			Single-input/single-output	
	$\sigma_{\text{USV}}$	$\sigma_{\text{SSV}}$	$\sigma_{\text{fit}}$	Lateral	Directional
$\sigma$	0.65	0.72	0.72		
Margins					
Gain, dB (rad/s)	8.5 (8)	11.5 (8)	11.5 (8)	18 (17)	13 (13)
Phase, deg (rad/s)	35	41	41	7 (2.5)	62 (4.5)

<sup>a</sup>These MIMO margins were obtained using the universal phase and gain relationship. The MIMO analysis allows for simultaneous independent variations, and the SISO analysis allows for one axis variation.

not feed much roll rate to the yaw axis. As a result, the SISO analysis method matched the MIMO singular value method. Note, however, that the SISO method allows for one axis variation at a time, and the actual aircraft control system operates with all the loops closed.

Because the analytical results matched the flight results very well, the flight minimum singular value method can be used as a measure of multiloop stability margins. Although the near-real-time analysis was not described in this paper, the time used to generate flight-determined minimum singular value was less than 30 s and is considered insignificant. These computation times are small enough to support near-real-time, multiloop stability margin analysis. The near-real-time capability would minimize the time required for envelope expansion of aircraft with multiloop control systems.

### Concluding Remarks

Multiloop stability margins were determined and analyzed for the X-29A aircraft from flight data using methods described in this paper. The flight results compared well with predicted stability margins and cross compared well with the single-loop frequency results. Analytical stability robustness was determined using unscaled structured and scaled structured singular value analyses. Flight-determined singular values were determined using closed-loop frequency responses. Data analysis comparing predictions based on both methods showed good correlation; however, the SSV method matched the flight minimum singular value more closely than the USV method. Predicted unscaled singular value minimums were always more conservative than those of the scaled structured singular values throughout the entire frequency range.

Predicted and flight-determined minimum eigenvalues of the return difference matrix were also examined. Sensitivity of the algorithm was evaluated by changing a feedback gain by  $\pm 20\%$ , and the stability margins were compared with the nominal gain results. The flight singular value analysis method is suitable for detecting changes in stability margins.

A control system can be sensitive to any or all of the following factors: crossfeed, gain and phase, and parameter and nonlinear perturbations. For the X-29A, the crossfeed and nonlinear elements were of minimum impact at low angles of attack. As a result, the classical SISO stability margins matched the MIMO method. The singular value MIMO stability margin methods are conservative but are not restricted to single-loop analysis limitations. Such multivariable robustness methods as real  $\mu$ -analysis need to be applied to further reduce the conservativeness.

Extracting multiloop singular values from flight data and comparing the information with prediction validates the use of flight singular values as a relative measure of robustness. This comparison increases the confidence of using structured singular values for stability assessments of multiloop control systems. This confidence is based on limited flight experience,

and more data, such as highly coupled and nonlinear control systems, need to be analyzed using MIMO methods. This method can be used on any multiloop control system. In addition, this technique extends the single-loop gain and phase margin concepts to multiloop systems. The methodology could be implemented in near real time for flight-monitoring and safety requirements. Near-real-time capability would minimize the time required for envelope expansion of aircraft with multiloop control systems.

### Acknowledgments

I would like to thank Marty Brenner, J. D. Paduano, and Anthony Pototzky for their technical input, helpful suggestions, and valuable comments on the topic of multivariable robustness.

### References

- <sup>1</sup>Doyle, J. C., and Stein, G., "Multivariable Feedback Design: Concepts for a Classical/ Modern Synthesis," *IEEE Transactions on Automatic Control*, Vol. AC-26, No. 1, 1981, pp. 4-16.
- <sup>2</sup>Ly, U., "Robustness Analysis of a Multiloop Flight Control System," *Proceedings of the AIAA Guidance and Control Conference* (Gatlinburg, TN), AIAA, New York, 1983, pp. 155-165 (AIAA Paper 83-2189).
- <sup>3</sup>Paduano, J. D., and Downing, D. R., "Application of a Sensitivity Analysis Technique to High-Order Digital Flight Control Systems," NASA CR-179429, Sept. 1987.
- <sup>4</sup>Newsom, J. R., and Mukhopadhyay, V., "A Multiloop Robust Controller Design Study Using Singular Value Gradients," *Journal of Guidance, Control, and Dynamics*, Vol. 8, No. 4, 1985, pp. 514-519.
- <sup>5</sup>Doyle, J. C., Wall, J. E., and Stein, G., "Performance and Robustness Analysis for Structured Uncertainty," *Proceedings of the 21st IEEE Conference on Decision and Control*, IEEE, New York, Vol. 2, Dec. 1982, pp. 629-636.
- <sup>6</sup>Pototzky, A. S., Wieseman, C. D., Hoadley, S. T., and Mukhopadhyay, V., "Development and Testing of Methodology for Evaluating the Performance of Multi-Input/Multi-Output Digital Control Systems," NASA TM-102704, Aug. 1990.
- <sup>7</sup>Gera, J., Bosworth, J. T., and Cox, T. H., "X-29A Flight Test Techniques and Results: Flight Controls," NASA TP-3121, May 1991.
- <sup>8</sup>Bosworth, J. T., "Flight-Determined Longitudinal Stability Characteristics of the X-29A Airplane Using Frequency Response Techniques," NASA TM-4122, June 1989.
- <sup>9</sup>Burken, J. J., "Flight-Determined Stability Analysis of Multiple-Input-Output Control Systems," NASA TM-4416, Nov. 1992.
- <sup>10</sup>Sefic, W. J., and Maxwell, C. M., "X-29A Technology Demonstrator Flight Test Program Overview," NASA TM-86809, April 1986.
- <sup>11</sup>Mukhopadhyay, V., and Newsom, J. R., "Application of Matrix Singular Value Properties for Evaluating Gain and Phase Margins of Multiloop Systems," AIAA Paper 82-1574, Aug. 1982.
- <sup>12</sup>Paduano, J. D., and Downing, D. R., "Sensitivity Analysis of Digital Flight Control Systems Using Singular-Value Concepts," *Journal of Guidance, Control, and Dynamics*, Vol. 12, No. 3, 1989, pp. 297-303.